Electronic Supplementary Information

Self-Powered Electrocatalytic Ammonia Synthesis Directly from Air as Driven by Dual Triboelectric Nanogenerators

Kai Han,[ab] Jianjun Luo,[ab] Yawei Feng,[ab] Liang Xu,[ab] Wei Tang*[abc] and Zhong Lin Wang*[abd]

[a]CAS Center for Excellence in Nanoscience, Beijing Institute of Nanoenergy and Nanosystems, Chinese Academy of Sciences, Beijing 100083, P. R. China
Email: tangwei@binn.cas.cn
[b]School of Nanoscience and Technology, University of Chinese Academy of Sciences, Beijing 100049, P. R. China
[c]Center on Nanoenergy Research, School of Physical Science and Technology, Guangxi University, Nanning 530004, P.R. China
[d]School of Material Science and Engineering, Georgia Institute of Technology, Atlanta, Georgia 30332-0245, USA.
Email: zlwang@gatech.edu

Table. S1 State of the art in electrocatalytic ammonia synthesis and our self-powered synthetic method.

Ref.	Anode	Cathode	T	P	Raw materials	Electrolyte	NH_3 yeild ($\mu g\ h^{-1}$)	Power
1	Pt sheet	Nanoporous Pd on a glassy carbon disk electrode (0.29 mg cm^{-2}, 0.28 cm^2)	Ambient conditions		N_2, H_2O	0.1 M PBS	1.66 (5.92 $\mu g\ h^{-1}\ cm^{-2}$) (20.4 $\mu g\ h^{-1}\ mg^{-1}$)	-0.15 V vs. RHE
2	Graphite plate	Au nanorods on a carbon paper (1 cm^2)	Ambient conditions		N_2, H_2O	0.1 M KOH	1.648 (1.648 $\mu g\ h^{-1}\ cm^{-2}$)	-0.2 V vs. RHE
3	Pt mesh	Au_6/Ni on a carbon cloth (2.0 mg cm^{-2}, 1 cm^2)	Ambient conditions		N_2, H_2O	0.05 M H_2SO_4	14.8 (14.8 $\mu g\ h^{-1}\ cm^{-2}$) (7.4 $\mu g\ h^{-1}\ mg^{-1}$)	-0.14 V vs. RHE
4	Pt foil	Au sub-nanoclusters/TiO_2 on a carbon paper (1 mg, 1 cm^2)	Ambient conditions		N_2, H_2O	0.1 M HCl	21.4 (21.4 $\mu g\ h^{-1}\ cm^{-2}$) (21.4 $\mu g\ h^{-1}\ mg^{-1}$)	-0.2 V vs. RHE
5	Pt foil	Fe-N-C on a carbon paper (1 mg cm^{-2}, 1 cm^2)	Ambient conditions		N_2, H_2O	0.1 M KOH	7.48 (7.48 $\mu g\ h^{-1}\ cm^{-2}$) (7.48 $\mu g\ h^{-1}\ mg^{-1}$)	0 V vs. RHE
6	Graphite rod	Cu/PI-300 on a carbon cloth (1 cm^2)	Ambient conditions		N_2, H_2O	0.1 M KOH	17.2 (17.2 $\mu g\ h^{-1}\ cm^{-2}$)	-0.4 V vs. RHE
7	Pt foil	Plasma R-O-Bi on a carbon paper	Ambient conditions		N_2, H_2O	0.2 M Na_2SO_4	2.4 (2.400 $\mu g\ h^{-1}\ cm^{-2}$)	-0.9 V vs. RHE

		(0.5 mg cm^{-2}, 1 cm^2)				(5.453 μg h^{-1} mg_{Bi}^{-1})	
8	Graphite rod	Fe-doped TiO_2 on a carbon paper (0.1 mg， 1 cm^2)	Ambient conditions	N_2, H_2O	0.5 M $LiClO_4$	2.547 (2.547 μg h^{-1} cm^{-2}) (25.47 μg h^{-1} mg^{-1})	-0.40 V vs. RHE
9	Pt foil	C-doped TiO_2 on a carbon paper (0.60 mg cm^{-2}, 1 cm^2)	Ambient conditions	N_2, H_2O	0.1 M $LiClO_4$	8.88 (8.88 μg h^{-1} cm^{-2}) (14.8 μg h^{-1} mg^{-1})	-0.4 V vs. RHE
10	Pt wire	WO_{3-x}(Vo)_H_2 on a carbon fiber paper (1.2 mg, 1 x 1.2 cm^2)	Ambient conditions	N_2, H_2O	PH=1, HCl	5.04 (4.2 μg h^{-1} cm^{-2}) (4.2 μg h^{-1} mg^{-1})	-0.12 V vs. RHE
11	Graphite rod	PC/Sb/$SbPO_4$ on a carbon paper (0.2 mg cm^{-2}, 1 cm^2)	Ambient conditions	N_2, H_2O	0.1 M HCl	5 (5 μg h^{-1} cm^{-2}) (25 μg h^{-1} mg^{-1})	-0.25 V vs. RHE
12	Graphite rod	Defect-rich MoS_2 on a carbon paper (0.1 mg, 0.5 x 0.5 cm^2)	Ambient conditions	N_2, H_2O	0.1 M Na_2SO_4	2.928 (11.712 μg h^{-1} cm^{-2}) (29.28 μg h^{-1} mg^{-1})	-0.4 V vs. RHE
13	Pt plate	Few-layer black Phosphorus nanosheets on a carbon fiber substrate (about 0.2 mg)	Ambient conditions	N_2, H_2O	0.01 M HCl	6.274 (31.37 μg h^{-1} mg^{-1})	-0.7 V vs. RHE
14	Pt foil	Eex-COF on a nitrogen-doped carbon nanosheet (1 mg, 1 cm^2)	Ambient conditions	N_2, H_2O	0.1M KOH	12.53 (12.53 μg h^{-1} cm^{-2}) (12.53 μg h^{-1} mg^{-1})	-0.2 V vs. RHE
15	Pt wire	MOF(Fe) on a carbon paper (1 x 3 cm^2)	90 °C AP	Air, H_2O	2 M KOH	279.1 (93.02 μg h^{-1} cm^{-2}) (1.52 x 10^{-9} mol s^{-1} cm^{-2})	1.2 V
16	$Pr_{0.6}Ba_{0.4}Fe_{0.8}Cu_{0.2}O_{3-\delta}$	$Pr_{0.6}Ba_{0.4}Fe_{0.8}Cu_{0.2}O_{3-\delta}$ (1.281 cm^2)	400 °C AP	Wet air (3 mol% H_2O)	$Ce_{0.8}Gd_{0.2}O_{2-\delta}$ (CGO)-(Li,Na,K)$_2CO_3$	8.4 (6.56 μg h^{-1} cm^{-2}) (1.07 x 10^{-6} mol s^{-1} m^{-2})	1.4 V
17	$La_{0.8}Cs_{0.2}Fe_{0.8}Ni_{0.2}O_{3-\delta}$	$La_{0.8}Cs_{0.2}Fe_{0.8}Ni_{0.2}O_{3-\delta}$ (1.281 cm^2)	600 °C AP	Wet air (3 mol% H_2O)	$Ce_{0.8}Gd_{0.2}O_{2-\delta}$ (CGO)-(Li,Na,K)$_2CO_3$	7.22 (5.64 μg h^{-1} cm^{-2}) (9.21 x 10^{-7} mol s^{-1} m^{-2})	1.4 V
18	30 wt% Pt/C on a gas diffusion layer	30 wt% Pt/C on a gas diffusion layer (1 mg cm^{-2}, 1 cm^2)	RT AP	Air, H_2O	solid electrolyte	69.77 (69.77 μg h^{-1} cm^{-2}) (1.14 x 10^{-5} mol m^{-2} s^{-1})	-1.6 V
19	30 wt% Pt/C on a carbon paper	30 wt% Pt/C on a carbon paper (1 cm^2)	80 °C ambient	Air, H_2O	0.1 M Li_2SO_4	57.34 (57.34 μg h^{-1} cm^{-2}) (9.37 x 10^{-6} mol m^{-2} s^{-1})	1.2 V
This	Graphite	TiO_2/carbon	Ambient	NO_3^-,	100 mg	1.9	-3 V

work	plate	cloth (1 mg cm^{-2}, 1 cm^2)	conditions	H_2O	L^{-1} NO_3^-		
	Graphite plate	TiO_2/carbon cloth (1 mg cm^{-2}, 1 cm^2)		NO_3^-, H_2O	100 mg L^{-1} NO_3^-	5.7	TENG (5000 r min^{-1})
	Graphite plate	TiO_2/carbon cloth (1 mg cm^{-2}, 1 cm^2)		NO_3^-, H_2O	100 mg L^{-1} NO_3^-	20.8	TENG with transformer (5000 r min^{-1})
	Graphite plate	TiO_2/carbon cloth (1 mg cm^{-2}, 2.5 x 2.5 cm^2)		Air, H_2O	mixed NO_3^- and NO_2^-	2.4	Self-powered (3.5 m^3 min^{-1})

Note: T, temperature. P, pressure. RT, room temperture. AP, atmospheric presssure. RHE, reversible hydrogen electrode. PBS, phosphate buffer solution. Eex-COF, Eletrochemically excitated covalent organic frameworks. PC, phosphorus-doped carbon.

References

1 W. Xu, G. Fan, J. Chen, J. Li, L. Zhang, S. Zhu, X. Su, F. Cheng, J. Chen, *Angew. Chem. Int. Ed.*, 2020, **59**, 3511-3516.
2 D. Bao, Q. Zhang, F.-L. Meng, H.-X. Zhong, M.-M. Shi, Y. Zhang, J.-M. Yan, Q. Jiang, X.-B. Zhang, *Adv. Mater.*, 2017, **29**, 1604799.
3 Z.-H. Xue, S.-N. Zhang, Y.-X. Lin, H. Su, G.-Y. Zhai, J.-Tan Han, Q.-Y. Yu, X.-H. Li, M. Antonietti, J.-S. Chen, *J. Am. Chem. Soc.*, 2019, **141**, 14976-14980.
4 M.-M. Shi, D. Bao, B.-R. Wulan, Y.-H. Li, Y.-F. Zhang, J.-M. Yan, Q. Jiang, *Adv. Mater.*, 2017, **29**, 1606550.
5 M. Wang, S. Liu, T. Qian, J. Liu, J. Zhou, H. Ji, J. Xiong, J. Zhong, C. Yan, *Nat. Commun.*, 2019, **10**, 341.
6 Y.-X. Lin, S.-N. Zhang, Z.-H. Xue, J.-J. Zhang, H. Su, T.-J. Zhao, G.-Y. Zhai, X.-H. Li, M. Antonietti, J.-S. Chen, *Nat. Commun.*, 2019, **10**, 4380.
7 Y. Wang, M. Shi, D. Bao, F. Meng, Q. Zhang, Y. Zhou, K. Liu, Y. Zhang, J. Wang, Z. Chen, D. Liu, Z. Jiang, M. Luo, L. Gu, Q. Zhang, X. Cao, Y. Yao, M. Shao, Y. Zhang, X.-B. Zhang, J. G. Chen, J. Yan, Q. Jiang, *Angew. Chem. Int. Ed.*, 2019, **58**, 9464-9469.
8 T. Wu, Z. Xing, S. Mou, C. Li, Y. Qiao, Q. Liu, X. Zhu, Y. Luo, X. Shi, Y. Zhang, X. Sun, *Angew. Chem. Int. Ed.*, 2019, **58**, 18449-18453.
9 Q. Qin, Y. Zhao, M. Schmallegger, T. Heil, J. Schmidt, R. Walczak, G. Gescheidt-Demner, H. Jiao, M. Oschatz, *Angew. Chem. Int. Ed.*, 2019, **58**, 13101-13106.
10 Z. Sun, R. Huo, C. Choi, S. Hong, T.-S. Wu, J. Qiu, C. Yan, Z. Han, Y. Liu, Y.-L. Soo, Y. Jung, *Nano Energy*, 2019, **62**, 869-875.
11 X. Liu, H. Jang, P. Li, J. Wang, Q. Qin, M. G. Kim, G. Li, J. Cho, *Angew. Chem. Int. Ed.*, 2019, **58**, 13329-13334.
12 X. Li, T. Li, Y. Ma, Q. Wei, W. Qiu, H. Guo, X. Shi, P. Zhang, A. M. Asiri, L. Chen, B. Tang, X. Sun, *Adv. Energy Mater.*, 2018, **8**, 1801357.
13 L. Zhang, L.-X. Ding, G.-F. Chen, X. Yang, H. Wang, *Angew. Chem. Int. Ed.*, 2019, **58**, 2612-2616.
14 S. Liu, M. Wang, T. Qian, H. Ji, J. Liu, C. Yan, *Nat. Commun.*, 2019, **10**, 3898.
15 X. Zhao, F. Yin, N. Liu, G. Li, T. Fan, B. Chen, *J. Mater. Sci.*, 2017, **52**, 10175-10185.
16 R. Lan, K. A. Alkhazmi, I. A. Amar, S. Tao, *Appl. Catal., B*, 2014, **152-153**, 212-217.
17 R. Lan, K. A. Alkhazmi, I. A. Amar, S. Tao, *Electrochim. Acta*, 2014, **123**, 582-587.
18 R. Lan, J. T. S. Irvine, S. Tao, *Sci. Rep.*, 2013, **3**, 1145.
19 R. Lan, S. Tao, *RSC Adv.,* 2013, **3**, 18016-18021.

Chemical Reagents

Hydrochloric acid (Beijing Chemical Works, HCl, 36.0-38.0%), ammonium sulfamate (Aladdin, $H_6N_2O_3S$, AR, 99.0%), sulfanilamide (Aladdin, $C_6H_8N_2O_2S$, standard for GC, >99.8%), N-(1-naphthy) ethylenediamine dihydrochloride (Aladdin, $C_{12}H_{14}N_2{\cdot}2HCl$, ACS, >98%), potassium nitrate (Aladdin, KNO_3, 99.99% metals basis), potassium nitrite (Aladdin, KNO_2, AR, 97%), sodium hydroxide (Beijing Chemical Works, NaOH, AR, 99%), salicylic acid (Aladdin, $C_7H_6O_3$, AR, 99.5%), sodium citrate dihydrate (MACKULIN, $Na_3C_6H_5O_7{\cdot}2H_2O$, AR, 99.0%), ammonium nitrate-15N (Aladdin, $NH_4{}^{15}NO_3$, 99atom%,

≥98.5%), sodium hypochlorite solution (Aladdin, NaClO, available chlorine, ≥5.0%), sodium nitroferricyanide dihydrate (Aladdin, $C_5FeN_6Na_2O \cdot 2H_2O$, 99.98% metals basis).

Determination of NO_3^-

A 5 mL of original or diluted solution is removed as the test sample. A 100 μL of 1 M HCl solution and a 400 μL of 5 wt% $H_6N_2O_3S$ aqueous solution are added into the sample in order, followed by 4.5 ml pure water. The mixed solution is measured by an ultraviolet-visible spectrophotometer (UV-3600, SHIMADZU Ltd.). The characteristic absorption of NO_3^- is at the wavelength of 210 nm. In addition, the absorbance at 275 nm is used to eliminate the potential interference. The absorbance calculation formula is as follows.

$$A_{NO_3^-} = A_{210} - 2 * A_{275}$$

Determination of NO_2^-

A 5 mL of original or diluted solution is removed as the test sample. A 100 μL of 10 g L^{-1} sulfanilamide solution containing 10% concentrated HCl solution is added into the sample. After 5 minutes, a 100 μL of 1 g L^{-1} $C_{12}H_{14}N_2 \cdot 2HCl$ is also added into to the sample. After 15 minutes, the mixed solution is measured. The characteristic absorption of NO_2^- is at the wavelength of 543 nm.

Determination of NH_3

NH_3 is determined by the indophenol blue method. A 2 mL of original or diluted solution is removed as the test sample. Then, a 2 mL of mixed solution containing 1 M NaOH, 5 wt% $C_7H_6O_3$ and 5 wt% $Na_3C_6H_5O_7$ is added into the sample, followed by a 1 mL of 0.05 mol L^{-1} NaClO and a 0.2 mL of 1 wt% $C_5FeN_6Na_2O$ solution. After 2 h, the solution is measured. The characteristic absorption of NH_3 is at the wavelength of 655 nm.

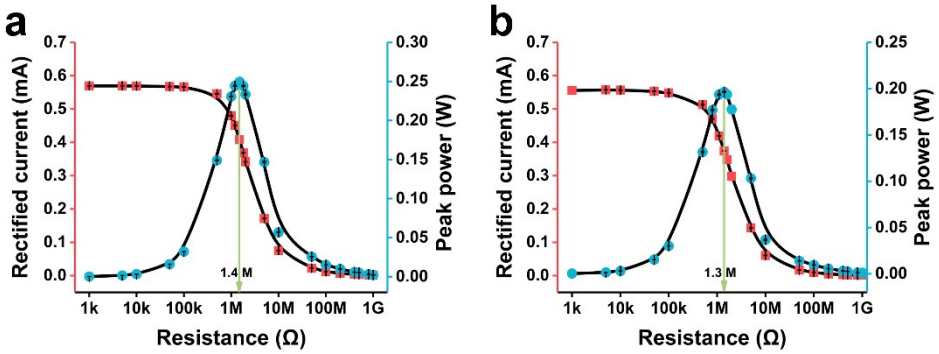

Fig. S1 Rectified current and peak power of (a) TENG-1 and (b) TENG-2.

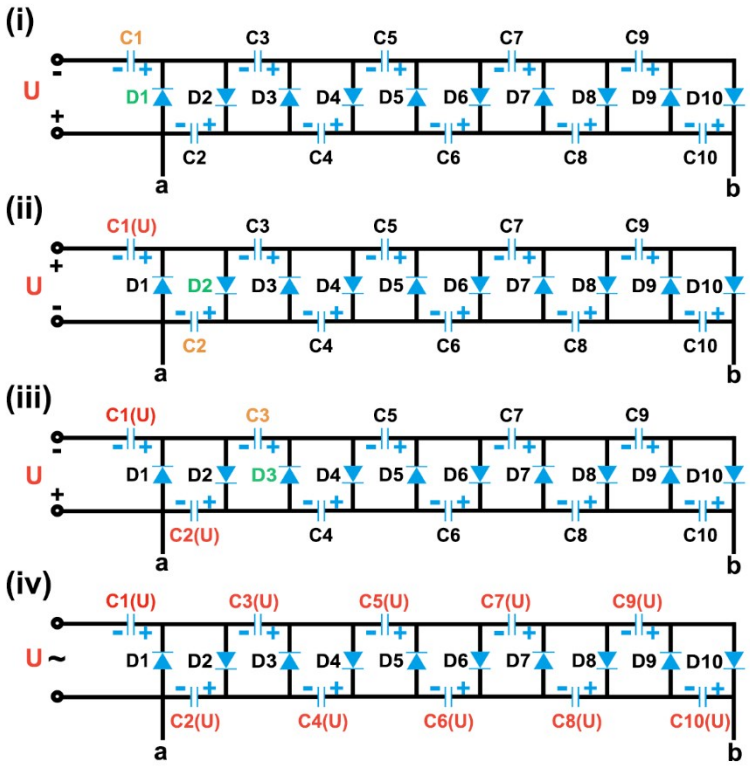

Fig. S2 Schematic diagram of the basic working principle of ten-stage voltage multiplier circuit.

Description of the principle

Since the output signal of TENG is alternating, diode D1 will be on and D2 will be off when the signal is in one half cycle as shown in the process (i). Meanwhile, capacitor C1 will be charged and the maximum voltage of C1 can reach to the same value U of TENG. In the process (ii), the output signal is in another half cycle, D2 will be on and D1 will be off. Similarly, Capacitor C2 can be charged with the maximum voltage value U. Then C3 and other capacitors will be charged gradually until all of them reach the same condition, as shown in process (iii) and (iv). Since each capacitor has the same voltage polarity, the voltage in the circuit is the sum of the voltages of ten capacitors. The voltage at end a is negative and end b is positive.

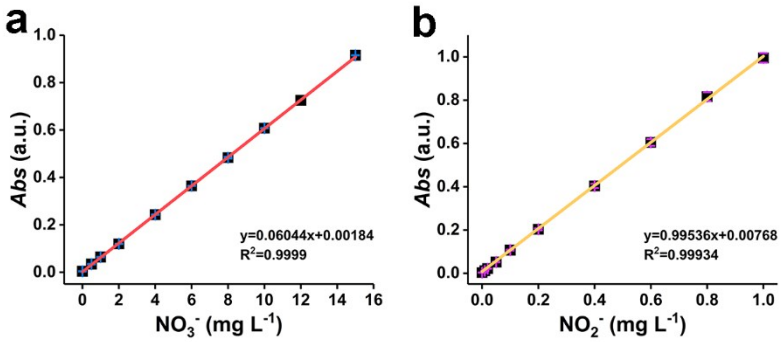

Fig. S3 Standard calibration curve of different concentrations of (a) NO_3^- and (b) NO_2^-.

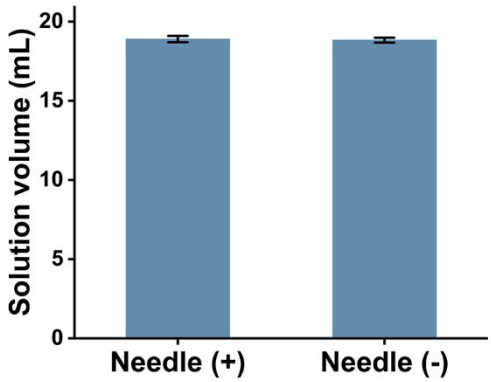

Fig. S4 Residual solution volume in the gas-washing bottle after 6 h air discharge when using needle as the positive or the negative electrode.

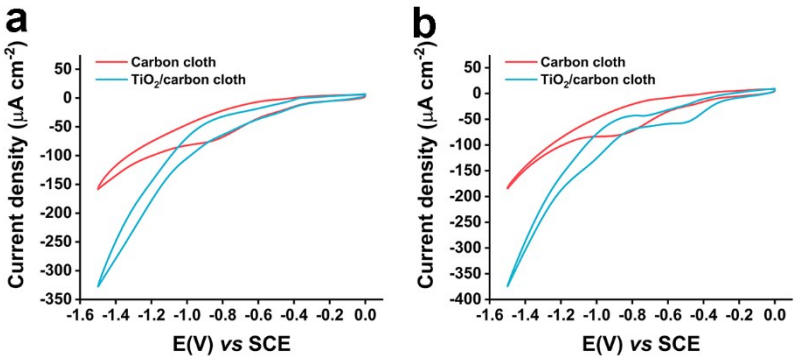

Fig. S5 CV curves in (a) 100 mg L^{-1} NO_3^- solution and (b) 100 mg L^{-1} NO_2^- solution.

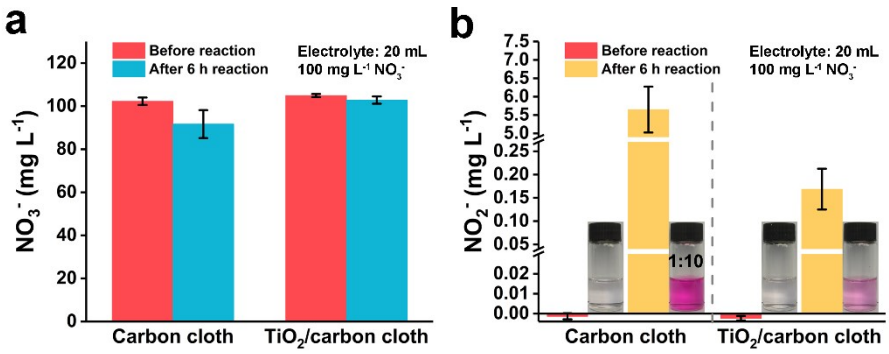

Fig. S6 Concentration variations of (a) NO_3^- and (b) NO_2^- using 100 mg L^{-1} NO_3^- as electrolyte in a single cell with a DC power (-3 V) drive.

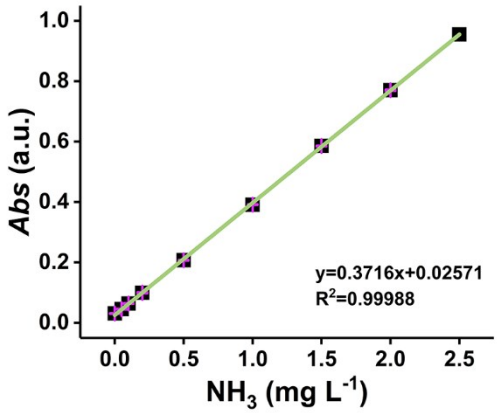

Fig. S7 Standard calibration curve of different concentrations of NH_3.

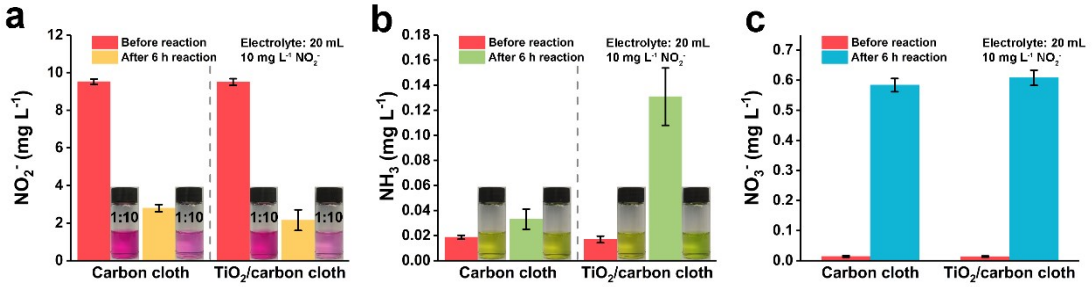

Fig. S8 Concentration variations of (a) NO_3^-, (b) NH_3 and (c) NO_2^- using 10 mg L^{-1} NO_2^- as electrolyte in a single cell with a DC power (-3 V) drive.

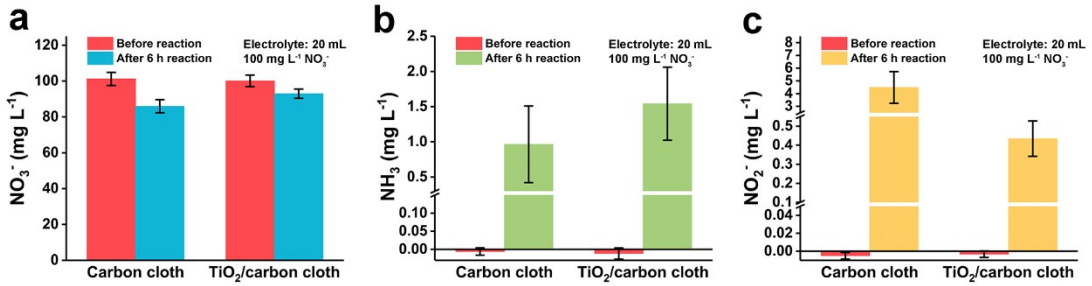

Fig. S9 Concentration variations of (a) NO_3^-, (b) NH_3 and (c) NO_2^- using 100 mg L^{-1} NO_3^- as electrolyte in a constant current condition with -0.25 mA by an electrochemical station.

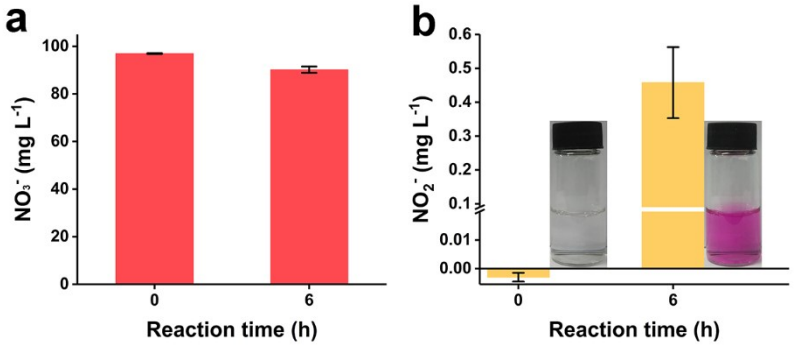

Fig. S10 Concentration variations of (a) NO_3^-, (b) NO_2^- using 100 mg L^{-1} NO_3^- as electrolyte in a single cell with rectified TENG-2 drive.

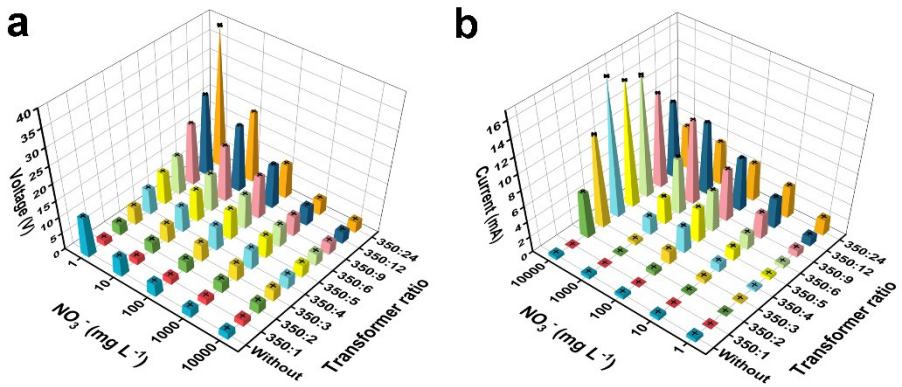

Fig. S11 (a) Voltage variation and (b) current variation of the single cell using different concentrations of NO_3^- with voltage regulating and rectified TENG-2 drive.

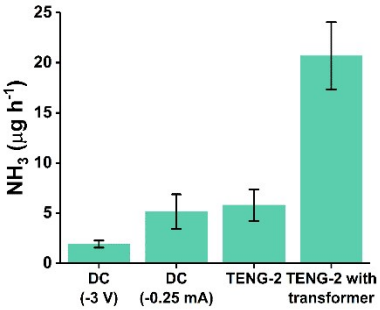

Fig. S12 Comparasion of NH_3 in mass yield per hour by DC (-3 V), DC (-0.25 mA), TENG-2 and TENG-2 with transformer.

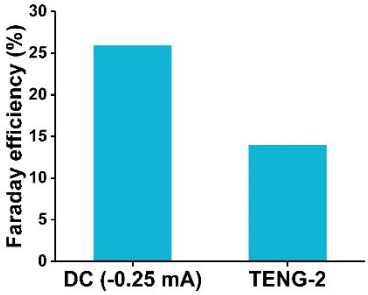

Fig. S13 Comparison of Faraday efficiency by DC (-0.25 mA) and TENG-2.

Calculation process

$$Faraday\ efficiency\ (\%) = \frac{mn_t tF}{\int_o^t idt} \times 100\%$$

m is the number of electrons of reducing NO_3^- into NH_3, n_t is the average mole yield per unit time of NH_3, t is the reaction time, F is Faraday constant, i is the current.

Since the output of TENG after rectification is pulsed signal, the current data are integrated.

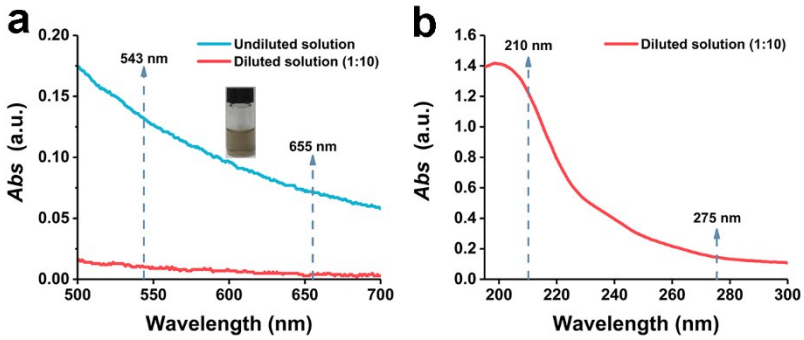

Fig. S14 Absorption curves in (a) ultraviolet and (b) visible region of electrolyte solution after 6 h reaction with or without dilution in a single cell driven by voltage step-down (350:12) and rectified TENG-2.

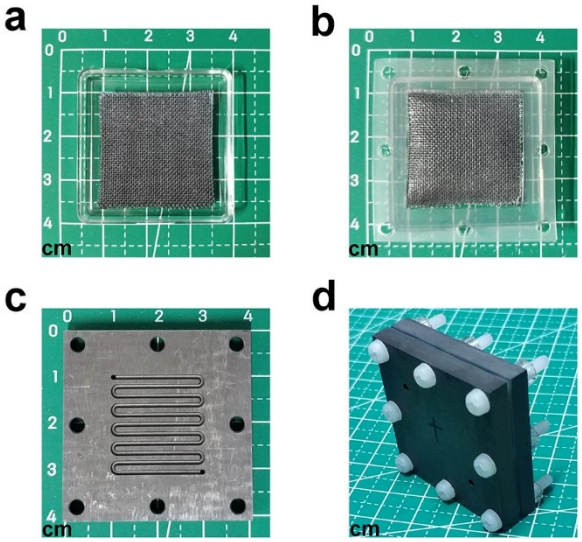

Fig. S15 Pictures of (a) a piece of TiO_2/carbon cloth, (b) an assembly of nafion membrane (NRE-211) and TiO_2/carbon cloth with silicone seal, (c) a graphite electrode and d) a dual-compartment electrocatalytic cell.

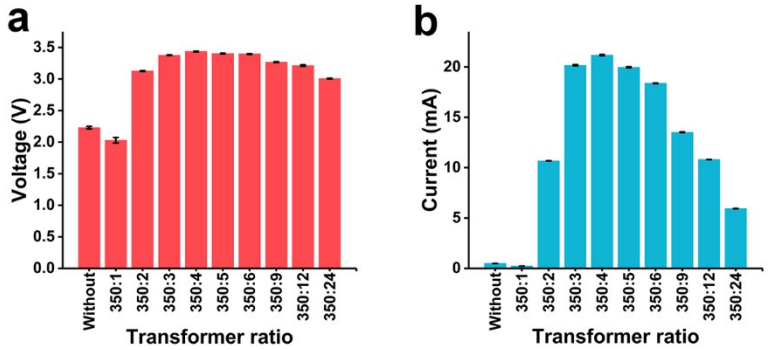

Fig. S16 (a) Voltage variation and (b) current variation of the dual-compartment electrocatalytic cell using 100 mg L^{-1} NO_3^- as electrolyte with voltage regulating and rectified TENG-2 drive.

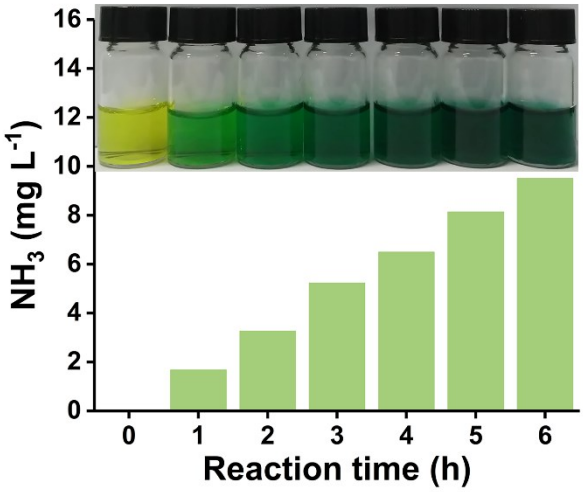

Fig. S17 Concentration variation of NH_3 from 1 to 6 h in the cathode with voltage step-down (350:4) and rectified TENG-2 drive.

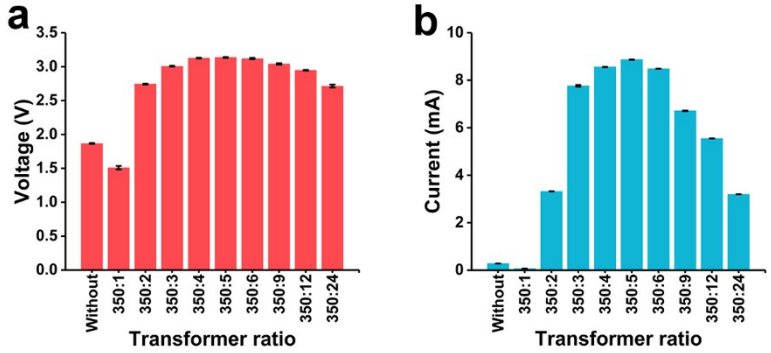

Fig. S18 (a) Voltage variation and (b) current variation of the dual-compartment electrocatalytic cell using electrolyte from air discharge with voltage regulating and rectified TENG-2 drive at a gas flow rate of 3.5 m^3 min^{-1}.

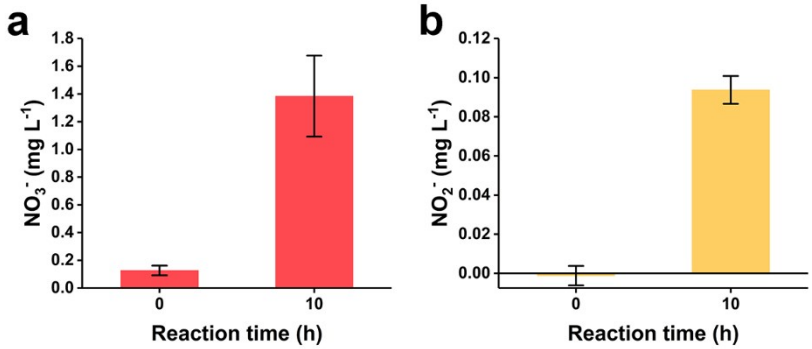

Fig. S19 (a) Concentration of NO_3^- in the cathode compartment by self-powered synthesis for 10 h. (b) Concentration of NO_2^- in the cathode compartment by self-powered synthesis for 10 h.